

## *Ab initio* Calculation of the Double Ionization of Helium in a Few-Cycle Laser Pulse Beyond the One-Dimensional Approximation

Camilo Ruiz,<sup>1</sup> Luis Plaja,<sup>1</sup> Luis Roso,<sup>1</sup> and Andreas Becker<sup>2</sup>

<sup>1</sup>*Departamento de Física Aplicada, Universidad de Salamanca, E-37008 Salamanca, Spain*

<sup>2</sup>*Max-Planck-Institut für Physik komplexer Systeme, Nöthnitzer Strasse 38, D-01187 Dresden, Germany*

(Received 7 October 2005; published 7 February 2006)

We present *ab initio* computations of the ionization of two-electron atoms by short pulses of intense linearly polarized Ti:sapphire laser radiation beyond the one-dimensional approximation. In the model the electron correlation is included in its full dimensionality, while the center-of-mass motion is restricted along the polarization axis. Our results exhibit a rich double ionization quantum dynamics in the direction transversal to the field polarization, which is neglected in the previous models based on the one-dimensional approximation.

DOI: 10.1103/PhysRevLett.96.053001

PACS numbers: 32.80.Rm, 33.80.Rv, 42.50.Hz

Electron correlation constitutes a basic resource for the understanding of the dynamics of many particle systems. Its relevance becomes particularly obvious in the double ionization of atoms by intense infrared laser radiation (for a recent review, see Ref. [1]). In the absence of electron correlation one would expect a sequential double ionization mechanism in which the electrons are emitted one after the other by their subsequent independent interaction with the external field. But, in experiments [2–4] it has been found that, in the low intensity range, the probabilities of double ionization by linearly polarized infrared lasers exceed the expectations based on this sequential mechanism by many orders of magnitude. The enhancement evidences the presence of an alternative mechanism of ionization of the two electrons, in which the correlation between the electrons plays an important role.

It is widely accepted now that the basic picture for the nonsequential ionization consists of the following three-step process [5–8]: First one electron is excited by the field to the continuum, afterwards it is accelerated by the field and rescatters with the second electron, which is excited in turn via a sharing of energy through electron-electron interaction. Recent differential measurements of ion and electron momenta and energies (e.g., Refs. [9–16]) have confirmed this nonsequential mechanism as being dominant for double ionization at intermediate intensities.

Despite the success of this picture, the *ab initio* calculation of the full dynamics of the two electrons driven by the field would potentially provide further quantitative insights into the process. Such computation of the double photoionization constitutes a major challenge, since it involves six dimensions in space and one in time. For the infrared frequencies of the widely used Ti:sapphire lasers at intensities of approximately  $10^{14}$  W/cm<sup>2</sup> it requires an extraordinary amount of computer resources [17,18]. Under these circumstances, the dimensional reduction of the many-body problem is a desirable strategy.

It has been shown that the fundamental aspects of the single-electron dynamics in linearly polarized strong fields

are retained in a 1D approach, in which the electron motion is restricted to the field polarization axis [19,20]. Stimulated by this successful application, the 1D reduction has been also employed for the two-electron [21,22], and, very recently, to the three-electron problem [23]. However, recent experimental data in laser induced double ionization of Ar revealed an emission of the electrons out off the polarization axis [14,16], attributed to the strong electron-electron repulsion after the two electrons left the atom on the same side. These observations suggest that for the ejection of two electrons the 1D approach may be less accurate than in the single-electron case. In this Letter we propose a new strategy that, preserving the full three dimensionality of the electronic relative coordinate, allows for *ab initio* computations at the wavelengths and intensities of Ti:sapphire lasers. The model is then applied to the double ionization of helium in an intense few-cycle pulse.

The Hamiltonian associated with the dynamics of the interaction of a two-electron atom or ion of charge  $Z_{\text{nucl}}$  with an electromagnetic wave can be written, in dipole approximation, as (Hartree atomic units,  $\hbar = m = e = 1$ , are used):

$$H(\mathbf{R}, \mathbf{r}, t) = \frac{\mathbf{P}^2}{4} + \mathbf{p}^2 - \frac{Z_{\text{nucl}}}{|\mathbf{R} + \frac{\mathbf{r}}{2}|} - \frac{Z_{\text{nucl}}}{|\mathbf{R} - \frac{\mathbf{r}}{2}|} + \frac{1}{r} - \frac{\mathbf{P} \cdot \mathbf{A}(t)}{c} \quad (1)$$

with  $\mathbf{R} = (\mathbf{r}_1 + \mathbf{r}_2)/2$  and  $\mathbf{P} = \mathbf{p}_1 + \mathbf{p}_2$ ;  $\mathbf{r} = \mathbf{r}_1 - \mathbf{r}_2$  and  $\mathbf{p} = (\mathbf{p}_1 - \mathbf{p}_2)/2$  are the center-of-mass and relative coordinates and associated momenta, respectively. Note that the field is coupled to the center-of-mass of the two electrons, but not to its relative coordinate. Therefore, for the case of linear polarization it is reasonable to restrict the center-of-mass motion to the field direction ( $\mathbf{P} \rightarrow P_Z$ ,  $\mathbf{R} \rightarrow Z$ ), while preserving the three-dimensional character of the electron-electron interaction.

Since for a linearly polarized field the total angular momentum along the polarization direction  $J_z = L_z + L_z$  remains unchanged, and  $m_z = 0$  as a result of the

dimensional reduction,  $L_z$  is invariant. Thus, the final model Hamiltonian has only 3 degrees of freedom, which can be chosen as the coordinates  $Z$ ,  $\rho$ , and  $z$  ( $\rho$  being the radius of the transversal relative coordinate):

$$H(Z, \rho, z, t) = \frac{p_Z^2}{4} + p_\rho^2 + p_z^2 + \frac{1}{\sqrt{\rho^2/4 + z^2}} - \frac{2}{\sqrt{\rho^2/4 + (Z + \frac{z}{2})^2 + a^2}} - \frac{2}{\sqrt{\rho^2/4 + (Z - \frac{z}{2})^2 + a^2}}, \quad (2)$$

where we have introduced a parameter  $a^2$  used in the computations to smooth the Coulomb singularity for the reduced electron-nucleus interactions.

In order to test the model we have performed computation of helium in an intense ultrashort laser pulse. The initial state wave function has been obtained by imaginary time propagation. Using  $a^2 = 0.135$  the ground state energies of the neutral helium and the helium ion are found to be equal to  $-2.936$  a.u. and to  $-1.985$  a.u., respectively. For the actual computations a four-cycle pulse having a pulse envelope of the form  $f(t) = \sin^2(\omega t/8)$  with a carrier frequency corresponding to the Ti:sapphire wavelength of 800 nm and a peak intensity of  $2.6 \times 10^{15}$  W/cm<sup>2</sup> has been considered. The wave function  $\Psi(Z, \rho, z; t)$  has been propagated using the Crank-Nicholson method with grid parameters  $\Delta\rho = \Delta z = \Delta Z = 0.3$  a.u. and  $N_\rho = 200$  and  $N_z = N_Z = 2000$  points; the time step was  $\Delta t = 0.05$  a.u. The calculation took about 20 days on a single processor machine.

Figure 1 shows the expectation value  $\langle \rho \rangle$  during the interaction. It offers clear evidence of the relevance of the transversal direction of the relative coordinate. The maxima of the oscillations coincide with the time instants at which the electric field is zero. Following the three-step model, these correspond to the times when the probability

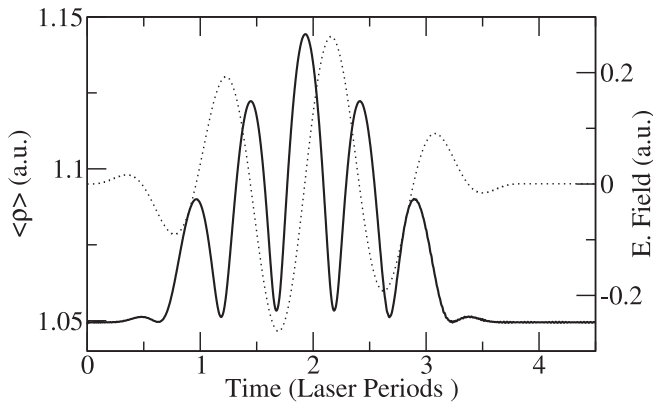


FIG. 1. Shown is the expectation value  $\langle \rho \rangle$  (solid line) as function of time along with the electric field (dotted line) at  $\lambda = 800$  nm and  $I_0 = 2.6 \times 10^{15}$  W/cm<sup>2</sup>.

of rescattering is high. In contrast, at time instants, where the field is at maximum and single ionization predominantly occurs,  $\langle \rho \rangle$  is at minimum and close to its initial value in the neutral atom. This demonstrates the marginal effect of electron correlation during single ionization as being a single-active-electron effect.

Figure 2 shows a panel of pictures corresponding to snapshots of the evolution of the probability distribution of the two-electron system during one laser period starting at  $t = 1T$ . Plots belonging to the left column show the probability distribution in the  $Z$ - $\rho$  space, integrated over the  $z$  coordinate. On the other hand, the plots in the right column offer the complementary view:  $Z$ - $z$  space integrated over  $\rho$ . The single ionized population is concentrated near the  $z_1$  and  $z_2$  axes (with  $z_1 = Z + z/2$  and  $z_2 = Z - z/2$ ), and the double ionized population extends over the regions in between these axes.

The panels in the first row [Figs. 2(a)] correspond to the time instant right after the interaction with the maximum field amplitude. As expected, these panels show the emission of single ionized wave packets along the  $z_1$  and  $z_2$  axes with  $Z < 0$ , i.e., in the direction of the field force. Note that in this case the population is confined to a region of small  $\rho$ , as one of the electrons still remains in the

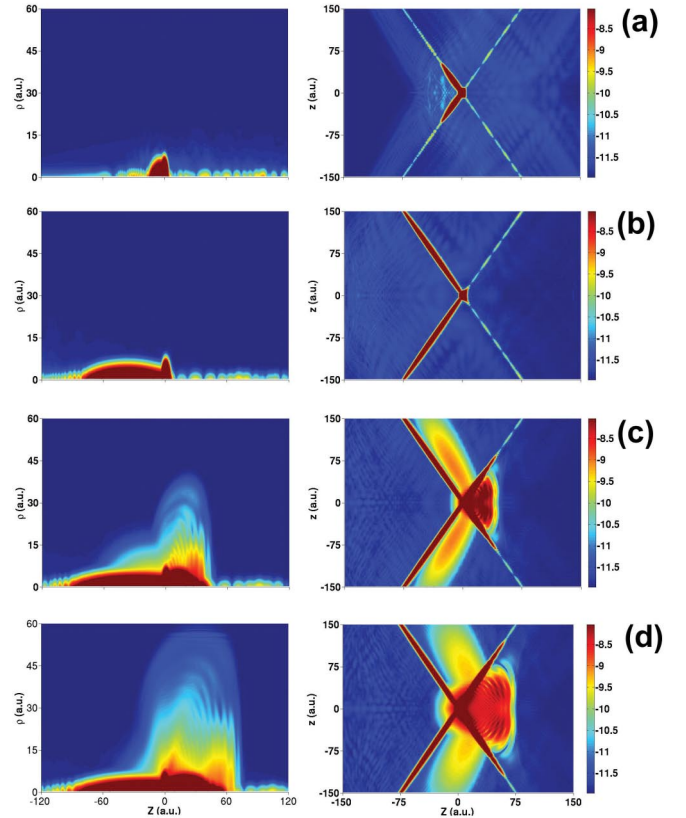


FIG. 2 (color online). Probability distributions at different time instants between  $t = 1T$  and  $t = 2T$ : (a)  $t = (1 + 6/16)T$ , (b)  $t = (1 + 10/16)T$ , (c)  $t = (1 + 14/16)T$ , and (d)  $t = (1 + 15/16)T$ . Left hand column:  $(Z, \rho)$  distributions, right hand column:  $(Z, z)$  distributions.

residual  $\text{He}^+$  ion. This is also in agreement with our interpretation of the results shown in Fig. 1, that electron correlation is negligible during single ionization.

According to the present understanding of the double ionization process, the single ionized electron acquires energy from the field before returning back to the parent ion. This excursion through the continuum corresponds to the situation depicted in Fig. 2(b), where the single ionized wave packets are almost at its turning points. Electron correlation is still negligible at this instant of time, as can be seen from the left hand panel in Fig. 2(b).

Figure 2(c) plots the situation at some time after the second field maximum. In contrast to the previous plots, in this snapshot the population shows a rich double ionization dynamics, in the longitudinal as well in the transversal directions. Indeed, one can identify two contributions (mechanisms) towards the double ionization region.

On the one hand there is a wave packet located near the axis origin, which extends towards the  $Z > 0$  direction (right triangle of the double ionization region in the right hand panel of Fig. 2(c)). It corresponds to the situation that two electrons are ejected at the same side of the nucleus. According to the three-step picture, this configuration is compatible with a nonsequential ionization process via electron-electron scattering. In agreement with the experimental observations [16], those electrons experience a strong transversal dynamics (c.f. left hand panel), which can be attributed to the Coulomb repulsion between the two electrons emitted to the same side. Previous *ab initio* models using the one-dimensional approximation for both electrons did not take account of this transversal dynamics.

There is a second wave packet released parallel to the  $z_1$  and  $z_2$  axes into the double ionization region (upper and lower triangle of the double ionization region). This corresponds to the ionization of a state, in which the first electron is found at some distance from the parent ion. Thus, this event corresponds to the field ionization of the singly ionized  $\text{He}^+$  ion. Since the field sign has been reversed from the single ionization event depicted in Fig. 2(a), the second electron is ionized in the opposite direction, i.e., forming an electron pair on opposite sides of the nucleus. Accordingly, the two electrons do not show such a strong transversal repulsion as in the first mechanism.

The latter contribution arises, most probably, from excited states of the ion, since we have found in test calculations that strong field ionization from the ground state of the ion is much less efficient than the sequential contribution observed in the present results. Thus, our results confirm earlier predictions [13,24] that excitation of the ion via rescattering followed by subsequent field ionization plays a decisive role in strong field double ionization.

The result of the sequential ionization can be traced as localized wave packets in the upper and lower triangles of the double ionization region of Figs. 2(c) and 2(d), showing that the mechanism is restricted to time instants just around

the field maximum. In contrast, the direct rescattering event underneath the double ionization occurs during a rather long time interval up to the zero of the field. Figs. 2(c) and 2(d) show how this broad wave packet is being gradually built, extending from the bound region into the right triangle of the double ionization region.

We note that the time delay between the maximum of the ejection of the single ionized wave packet and the maximum of the nonsequential ionization upon direct rescattering is about  $0.68T$  which is close to the corresponding limiting (high-intensity) value of  $0.75T$  found in the full 6D computations [18]. The difference may arise due to the different pulse shape used in the computations and/or the approximation of the center-of-mass motion along the polarization direction in the present model.

In Fig. 2(d) one further observes a ring structure in the contribution to double ionization created via direct rescattering, both in the  $(Z, \rho)$  as well as in the  $(Z, z)$  presentation. This structure becomes even more evident in the cuts over the three-dimensional probability distribution at the same time instant, shown in Fig. 3(a). The horizontal plane in this figure corresponds to the slice with  $\rho = 0$ , while the vertical planes are cuts at  $Z = 0$  and  $z = 0$ . A series of rings, which are parts of shells, and a pronounced angular structure are observed in all planes, mostly for  $z = 0$ .

This modulation in the double ionization population may indicate interferences between different paths in direct nonsequential double ionization. Such interference phenomena have been reported recently from numerical simulations of single ionization of hydrogen atom [25,26], which have been related to fringes in high resolution fully differential experimental data [27]. The latter effect is also visible in the single ionization region of the present data (see enlarged view in Fig. 3(b)). Indeed, it appears that the rings in the  $\rho = 0$  plane of the double ionization region are connected with the maxima in the single ionization region, indicating a related origin of the structures in the single and double ionization region.

Finally, in Fig. 4 we present the distribution of the center-of-mass momentum along the polarization direction,  $P_Z$ , in the region of double ionization at a zero of the field near the end of the pulse at  $t = 14/4T$ .

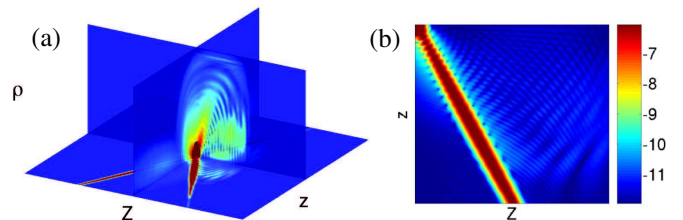


FIG. 3 (color online). (a) Slices of the three-dimensional probability distribution. The horizontal plane corresponds to  $\rho = 0$ , vertical planes are planes at  $Z = 0$  and  $z = 0$ . (b) Enlarged view, which shows the interference patterns in the single and double ionization region. This snapshot is taken at  $t = (1 + 15/16)T$ .

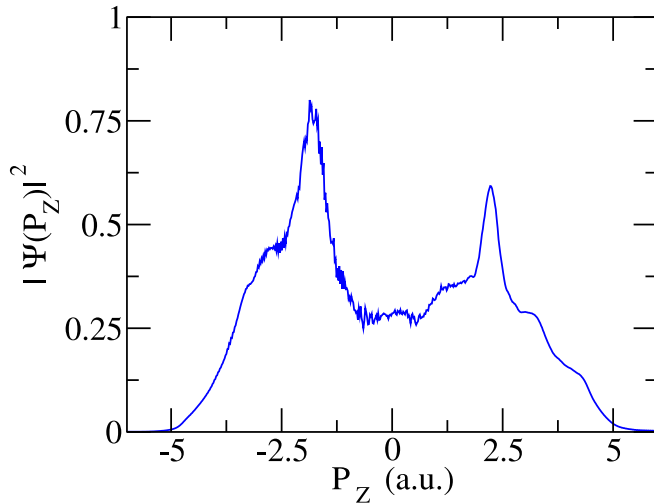


FIG. 4 (color online). Distribution of the center-of-mass momentum along the polarization direction in the double ionization region.

In order to calculate the distribution, we have adopted the method of partitions of the coordinate space as employed in earlier works [18]:

$$r_1 < 12 \text{ a.u.} \quad \text{and} \quad r_2 < 12 \text{ a.u.} : \text{He atom} \quad (3)$$

$$r_1 < 6 \text{ a.u.} \quad \text{and} \quad r_2 \geq 12 \text{ a.u.} \quad \text{or}$$

$$r_1 \geq 12 \text{ a.u.} \quad \text{and} \quad r_2 < 6 \text{ a.u.} : \text{He}^+ \text{ ion} \quad (4)$$

$$\text{complementary space} : \text{He}^{2+} \text{ ion} \quad (5)$$

with  $r_1 = \sqrt{(Z + \frac{z}{2})^2 + \frac{\rho^2}{4}}$  and  $r_2 = \sqrt{(Z - \frac{z}{2})^2 + \frac{\rho^2}{4}}$ .

The result in Fig. 4 is directly related to the first differential measurements [9,10] of the recoil ion momentum. The distribution shows the characteristic double hump structure with a central minimum. The maxima appear at about 2 a.u. and the distribution drops rapidly around the maximum allowed energy classically in a few-cycle pulse. The asymmetry in the height of the peaks arises because of the few-cycle pulse used in the calculations [28,29], but is also due to partial absorption of the double ionization population at the edges of the grid in the  $\rho$  direction near the end of the computations.

In conclusion, detailed *ab initio* calculations of the interaction of a strong infrared electromagnetic field with a helium atom beyond the one-dimensional approximation are presented. The model preserves the full dynamics of the two electrons in their relative coordinate, while it restricts the center-of-mass motion along the polarization direction.

The results show that the relevant aspects of the ionization dynamics in and out of the polarization axis are in

good agreement with the available experimental results. Our computations clearly demonstrate the multidimensional and the multiple path nature of nonsequential double ionization.

This work has been partially supported by the Spanish Ministerio de Ciencia y Tecnología (FEDER funds, Grant No. BFM2002-00033).

- 
- [1] A. Becker, R. Dörner, and R. Moshhammer, *J. Phys. B* **38**, S753 (2005).
  - [2] A. L'Huillier, L. A. Lompre, G. Mainfray, and C. Manus, *Phys. Rev. Lett.* **48**, 1814 (1982).
  - [3] B. Walker *et al.*, *Phys. Rev. Lett.* **73**, 1227 (1994).
  - [4] S. Larochelle, A. Talebpour, and S.L. Chin, *J. Phys. B* **31**, 1215 (1998).
  - [5] M. Yu. Kuchiev, *JETP Lett.* **45**, 404 (1987); *J. Phys. B* **28**, 5093 (1995).
  - [6] K.J. Schafer, B. Yang, L. F. DiMauro, and K. C. Kulander, *Phys. Rev. Lett.* **70**, 1599 (1993).
  - [7] P. B. Corkum, *Phys. Rev. Lett.* **71**, 1994 (1993).
  - [8] A. Becker and F.H.M. Faisal, *J. Phys. B* **29**, L197 (1996); *J. Phys. B* **38**, R1 (2005).
  - [9] Th. Weber *et al.*, *Phys. Rev. Lett.* **84**, 443 (2000).
  - [10] R. Moshhammer *et al.*, *Phys. Rev. Lett.* **84**, 447 (2000).
  - [11] Th. Weber *et al.*, *Nature (London)* **405**, 658 (2000).
  - [12] R. Lafon *et al.*, *Phys. Rev. Lett.* **86**, 2762 (2001).
  - [13] B. Feuerstein *et al.*, *Phys. Rev. Lett.* **87**, 043003 (2001).
  - [14] M. Weckenbrock *et al.*, *Phys. Rev. Lett.* **91**, 123004 (2003).
  - [15] R. Moshhammer *et al.*, *J. Phys. B* **36**, L113 (2003).
  - [16] M. Weckenbrock *et al.*, *Phys. Rev. Lett.* **92**, 213002 (2004).
  - [17] J.S. Parker, L.R. Moore, D. Dundas, and K.T. Taylor, *J. Phys. B* **33**, L691 (2000).
  - [18] J.S. Parker, B.J.S. Doherty, K.J. Meharg, and K.T. Taylor, *J. Phys. B* **36**, L393 (2003).
  - [19] Q. Su and J.H. Eberly, *Phys. Rev. A* **44**, 5997 (1991).
  - [20] R. Grobe and J.H. Eberly, *Phys. Rev. Lett.* **68**, 2905 (1992).
  - [21] M. Lein, E.K.U. Gross, and V. Engel, *Phys. Rev. Lett.* **85**, 4707 (2000).
  - [22] R. Panfili, S.L. Haan, and J.H. Eberly, *Phys. Rev. Lett.* **89**, 113001 (2002).
  - [23] C. Ruiz, L. Plaja, and L. Roso, *Phys. Rev. Lett.* **94**, 063002 (2005).
  - [24] R. Kopold, W. Becker, H. Rottke, and W. Sandner, *Phys. Rev. Lett.* **85**, 3781 (2000).
  - [25] D. Bauer, *Phys. Rev. Lett.* **94**, 113001 (2005).
  - [26] D.G. Arbó *et al.*, [quant-ph/0507131](http://arxiv.org/abs/quant-ph/0507131).
  - [27] A. Rudenko *et al.*, *J. Phys. B* **37**, L407 (2004).
  - [28] X. Liu and C. Figueira de Morisson Faria, *Phys. Rev. Lett.* **92**, 133006 (2004).
  - [29] X. Liu *et al.*, *Phys. Rev. Lett.* **93**, 263001 (2004).